

Astos Solutions GmbH

The Circular Restricted Three Body Problem and Numerical Approaches for Halo Orbit Propagation

Victor Hertel

April 27, 2018

Contents

1	Orbit Types in cis-lunar Space	3
1.1	Keplerian Orbits	3
1.1.1	Low Lunar Orbit (LLO)	3
1.1.2	Elliptical Lunar Orbit (ELO)	3
1.1.3	Frozen Lunar Orbit	3
1.2	Libration Point Orbits	3
1.2.1	Periodic Orbits	4
1.2.2	Quasi-Periodic Orbits	5
2	Classification of Halo Orbits	7
2.1	Halo Orbit Families	7
2.1.1	L_1 Halo Family	8
2.1.2	L_2 Halo Family	9
2.2	Near Rectilinear Halo Orbits (NRHOs)	10
3	Dynamical Models	11
3.1	n -Body Problem	11
3.2	Three Body Problem	11
3.3	Circular Restricted Three Body Problem	12
3.3.1	Assumptions	12
3.3.2	Coordinate Systems	12
3.3.3	Non-dimensionalization	13
3.3.4	Equations of Motion	13
3.3.5	Jacobi Constant	15

3.4	First Order Analytical Approximations for Motion in the Vicinity of Libration Points	15
3.5	Approximate Periodic Solutions	16
4	Dynamical Systems Theory	17
4.1	State Transition Matrix	17
4.2	Differential Corrections	18
4.3	Periodic Halo Orbit Computation	20
4.4	Continuation of an Halo Orbit Family	21
4.4.1	Natural Parameter Continuation	21
4.4.2	Pseudo-Arclength Continuation	22
	References	23

List of Figures

1	Tree structure of libration point orbits	4
2	Periodic orbits around L_2 libration point	4
3	Distant Retrograde Orbit around Europa	5
4	Quasi-periodic orbits around L_2 libration point	5
5	All the periodic and quasi-periodic orbits around L_2 libration point	6
6	L_1 and L_2 southern halo families [1]	7
7	Northern L_1 family, x-y projection, $\mu = 0.04$ [2]	8
8	Northern L_1 family, x-z projection, $\mu = 0.04$ [2]	8
9	Northern L_1 family, y-z projection, $\mu = 0.04$ [2]	8
10	Northern L_2 family, x-y projection, $\mu = 0.04$ [2]	9
11	Northern L_2 family, x-z projection, $\mu = 0.04$ [2]	9
12	Northern L_2 family, y-z projection, $\mu = 0.04$ [2]	9
13	Earth-Moon L_1 and L_2 halo stability indices [3]	10
14	Earth-Moon L_1 (right) and L_2 (left) halo stability indices [1]	10
15	Bounds of NRHOs	11
16	L_1 and L_2 northern and southern NRHOs [3]	11
17	Reference frames and position vectors in the CR3BP [4]	12
18	Linear variations relative to a reference trajectory $\bar{x}(t)$	19

List of Tables

1	Geometric dependencies of L_1 and L_2 halo families	9
2	Orbital characteristics of NRHOs	10

1 Orbit Types in cis-lunar Space

Orbits in cis-lunar space can be divided into **Keplerian Orbits** and **Libration Point Orbits**. Different orbit families of these subdivisions will be briefly presented in 1.1 and 1.2.

1.1 Keplerian Orbits

Keplerian Orbits are solutions of the two-body problem of celestial mechanics, which describe the motion of two bodies about their common barycenter. The motion forms a two-dimensional orbital plane in three-dimensional space in the shape of conic sections: circle, ellipse, parabola or hyperbola, depending on the orbital eccentricity ϵ .

1.1.1 Low Lunar Orbit (LLO)

Low Lunar Orbits (LLOs) are specific Keplerian orbits with an altitude around 100 km above the lunar surface. They were used as phasing orbits for surface access in the Apollo missions, as they represent good staging orbits to the surface.

1.1.2 Elliptical Lunar Orbit (ELO)

The Elliptical Lunar Orbit (ELO) is as well a specific Keplerian orbit. It offers potential lower cost access from Earth and with a low perilune over the lunar surface a favorable surface access.

1.1.3 Frozen Lunar Orbit

By careful selection of the orbital parameters, the natural drifting due to irregularities of the central body's shape can be minimized. Specifically, changes in the inclination, eccentricity and energy can be minimized by choosing initial values so that their perturbations cancel out. This results in a long-term stable orbit. NASA has identified four frozen lunar orbits at 27° , 50° , 76° and 86° inclination.

1.2 Libration Point Orbits

Orbits in the vicinity of the collinear libration points can be divided into families of periodic and families of quasi-periodic orbits. In the following explanation the L_2 libration point is used as an example. The results can be transferred to other collinear libration points. The subsubsection 1.2.1 and subsubsection 1.2.2 come from source [5].

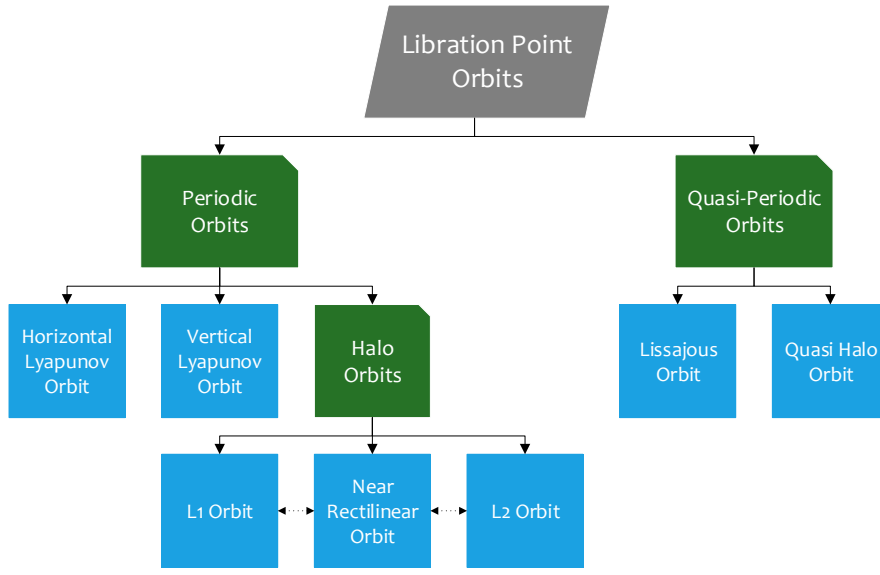


Figure 1: Tree structure of libration point orbits

1.2.1 Periodic Orbits

For energy values close to that at L_2 , where it is sufficient to consider only the linear approximation to the equations of motion, there exist two families of periodic orbits; the **Horizontal Lyapunov orbits**, which are in the ecliptic plane, and the horizontally symmetric figure-eight-shaped **Vertical Lyapunov orbits**. As the energy is increased, and nonlinear terms become important, the linear phase space is broken and a new periodic family, **Halo orbits**, bifurcate from the Horizontal Lyapunov orbit family. These orbits are three-dimensional and asymmetric about the ecliptic plane. Figure 2 shows the three distinct periodic orbit families around L_2 .

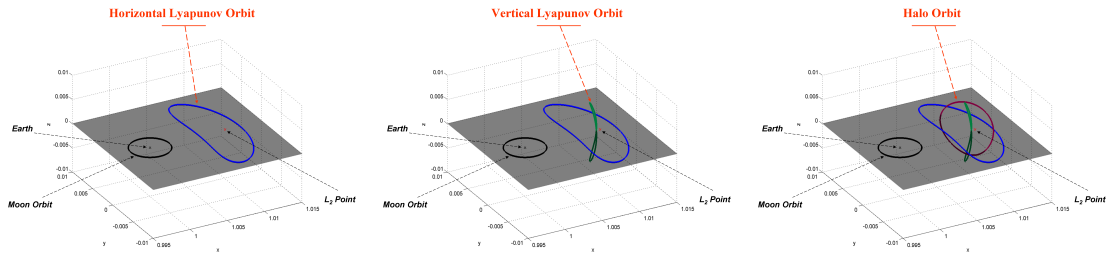


Figure 2: Periodic orbits around L_2 libration point

Distant Retrograde Orbit (DRO)

The lunar Distant Retrograde Orbit (DRO) is a highly stable orbit in the circular restricted

three body problem. In the rotating frame, the DRO looks like a large quasi-elliptical retrograde orbit around the Moon when in fact it orbits the Earth. Figure 3 shows a DRO seen from an inertial frame in the left plot and seen from the L_1 rotating frame in the right plot. [6]

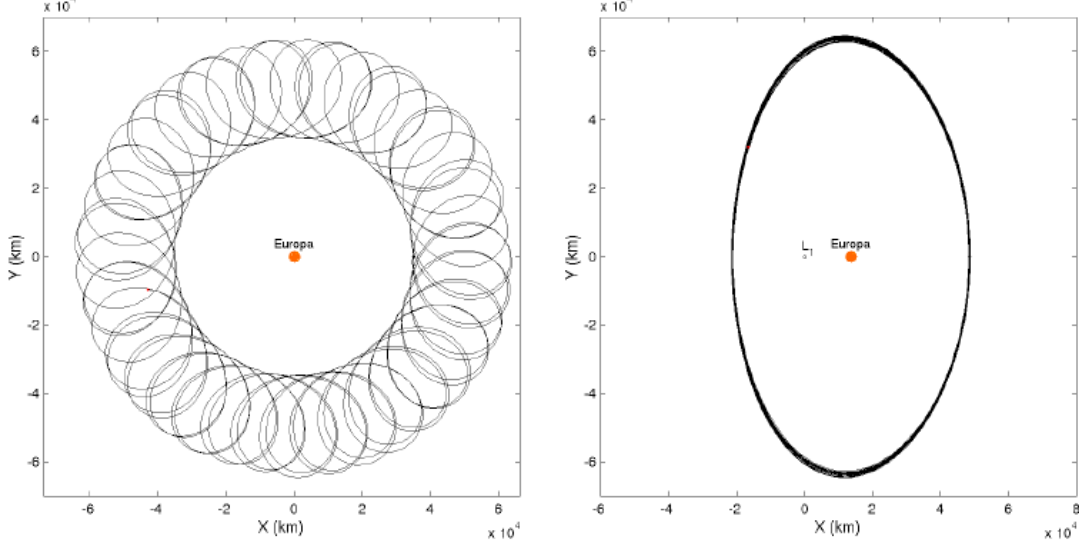


Figure 3: Distant Retrograde Orbit around Europa

1.2.2 Quasi-Periodic Orbits

The four-dimensional center manifold around L_2 is occupied by quasi-periodic orbits of two different families: The **Lissajous family** around the Vertical Lyapunov orbits, and the **Quasi-Halos** around the Halo orbits. These quasi-periodic orbits reside on invariant tori about the corresponding periodic orbit.

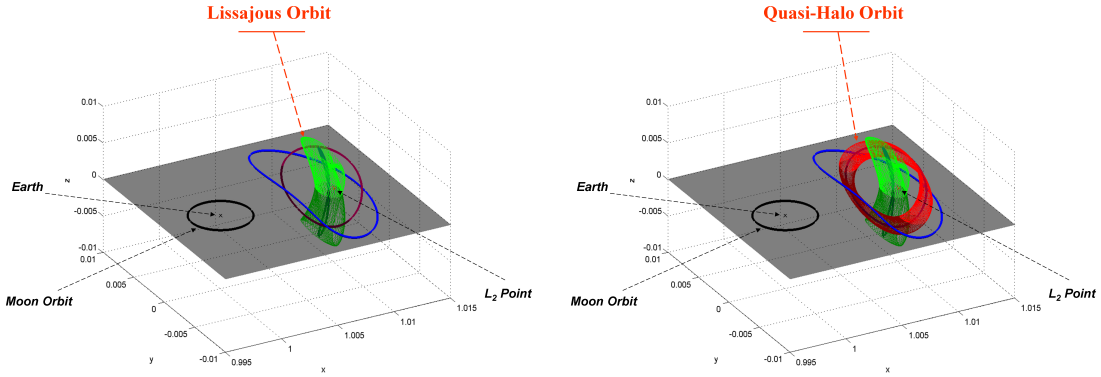


Figure 4: Quasi-periodic orbits around L_2 libration point

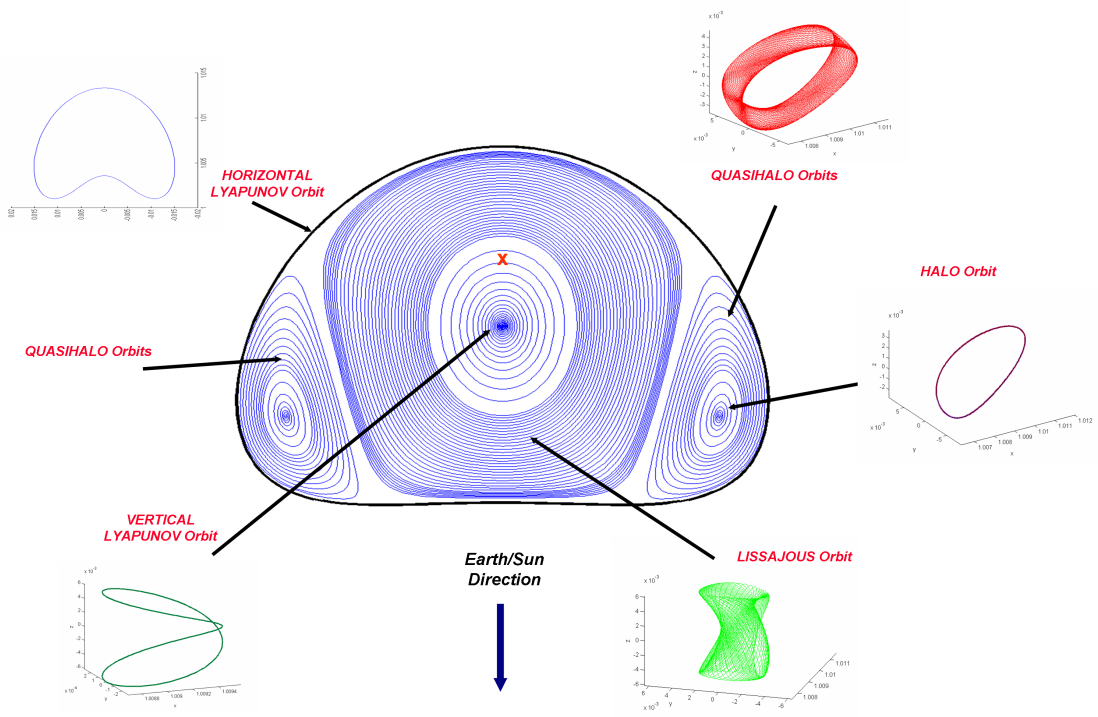


Figure 5: All the periodic and quasi-periodic orbits around L_2 libration point

2 Classification of Halo Orbits

2.1 Halo Orbit Families

Halo orbits are periodic, three-dimensional orbits near the collinear libration points L_1 , L_2 and L_3 . With respect to a rotating frame, where the unit vector \hat{x} is aligned with both primaries, \hat{y} is perpendicular to \hat{x} and in the plane of primary motion and $\hat{z} = \hat{x} \times \hat{y}$, they are symmetric across the $\hat{x}\hat{z}$ -plane. Every periodic halo orbit includes an out-of-plane component. This characteristic allows to divide the orbits into families [4]:

- **Northern Halo Family**
Orbits with a maximum out-of-plane excursion in the positive \hat{z} -direction labeled as *northern halo family*
- **Southern Halo Family**
Orbits with a maximum out-of-plane excursion in the negative \hat{z} -direction labeled as *southern halo family*

Depending on the encircled libration point, they can also be divided into L_1 Halo Family, L_2 Halo Family and L_3 Halo Family. Halo orbits exist near all three collinear libration points at a wide range of mass ratios.

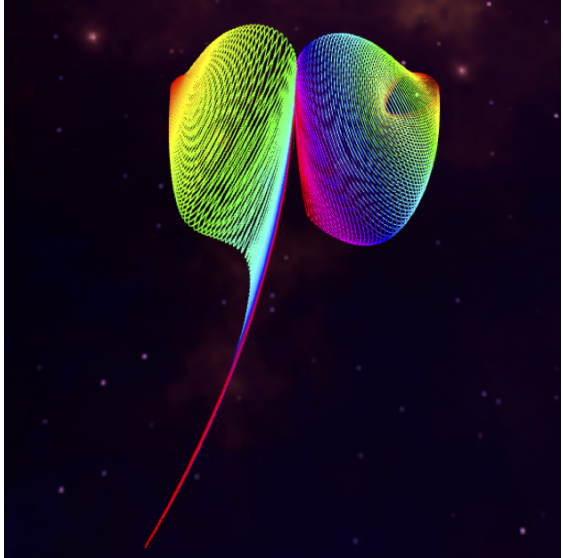


Figure 6: L_1 and L_2 southern halo families [1]

The stability characteristics are indicated by the stability index

$$\nu = \frac{1}{2} \left(\lambda_{max} + \frac{1}{\lambda_{max}} \right). \quad (1)$$

λ_{max} is the maximum eigenvalue of the state transition matrix (STM) of the halo orbit after precisely one revolution, also known as the monodromy matrix [3]. For a given orbit, stability is indicated if

$$|\nu_i| \leq 1, \quad i = 1, 2 \quad (2)$$

and ν_i is real. In the following sections these three families will be compared and geometric dependencies of the orbits briefly discussed. [2]

2.1.1 L_1 Halo Family

Three different perspectives of the northern L_1 halo family are shown in Figure 7, Figure 8 and Figure 9 with a given mass ratio $\mu = 0.04$. The region of stable orbits is bounded by the dashed orbits.

Increasing μ moves the stable orbits closer to the libration point until they disappear at $\mu \cong 0.0573$. It also increases the out-of-plane motion, thus making the orbits larger. [2]

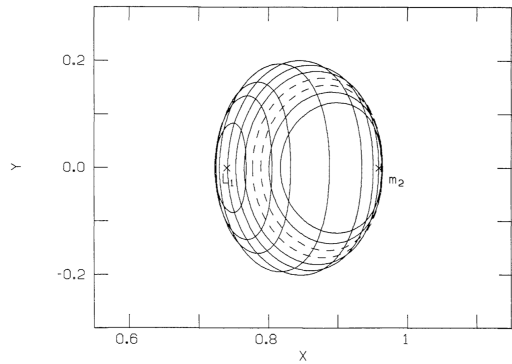


Figure 7: Northern L_1 family, x-y projection,
 $\mu = 0.04$ [2]

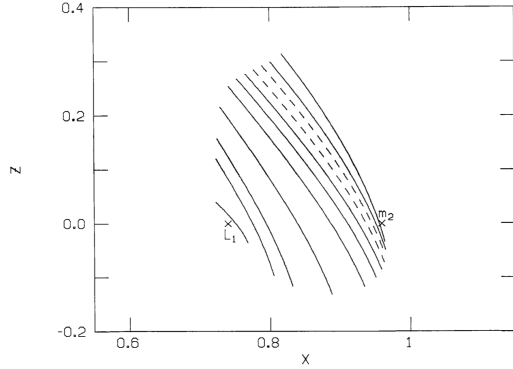


Figure 8: Northern L_1 family, x-z projection,
 $\mu = 0.04$ [2]

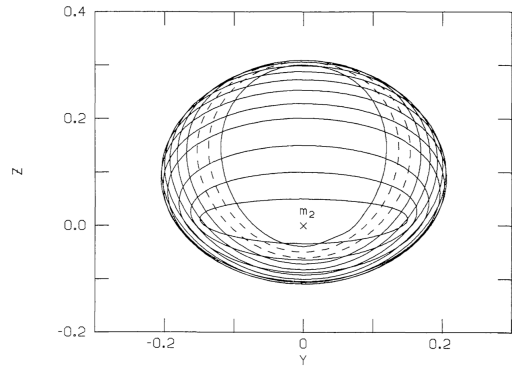


Figure 9: Northern L_1 family, y-z projection,
 $\mu = 0.04$ [2]

2.1.2 L_2 Halo Family

Three different perspectives of the northern L_2 halo family are shown in Figure 10, Figure 11 and Figure 12 with a given mass ratio $\mu = 0.04$. As before, the region of stable orbits is bounded by the dashed orbits.

Stable halo orbits near L_2 exist for all values of μ . Increasing the mass ratio moves the also increasing zone of stable orbits closer to m_2 rather than the libration point. As it was the case with L_1 , large values μ have more out-of-plane motion. The size of orbits is comparable to those near L_1 . [2]

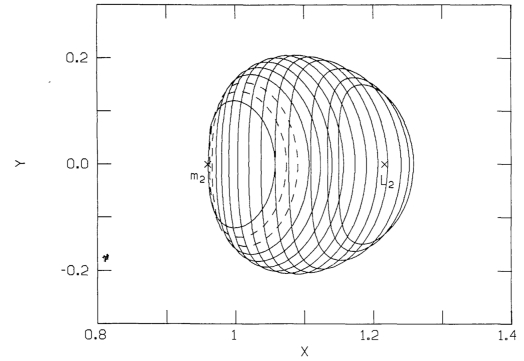


Figure 10: Northern L_2 family, x-y projection, $\mu = 0.04$ [2]

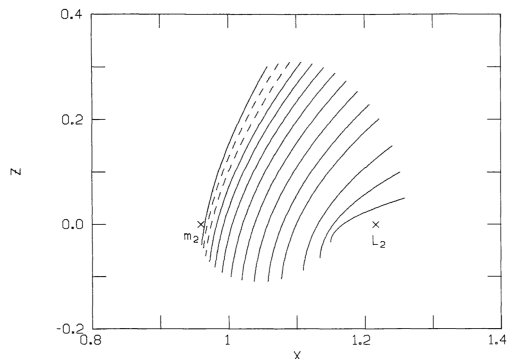


Figure 11: Northern L_2 family, x-z projection, $\mu = 0.04$ [2]

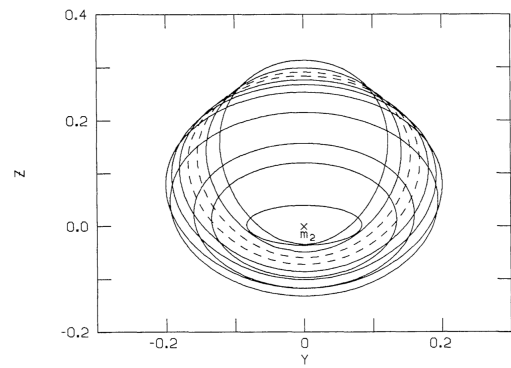


Figure 12: Northern L_2 family, y-z projection, $\mu = 0.04$ [2]

	L1	L2
$\mu \uparrow$	Stabil orbits $\rightarrow L_1$	Stabil orbits $\rightarrow m_2$
	Out-of-plane motion \uparrow	Out-of-plane motion \uparrow
	Orbit size \uparrow	Orbit size \uparrow

Table 1: Geometric dependencies of L_1 and L_2 halo families

2.2 Near Rectilinear Halo Orbits (NRHOs)

Near Rectilinear Halo Orbits (NRHOs) are defined as the subsection of the halo orbit family possessing stability indices all within some small bound surrounding ± 1 and with no stability index that is significantly larger in magnitude than the others.

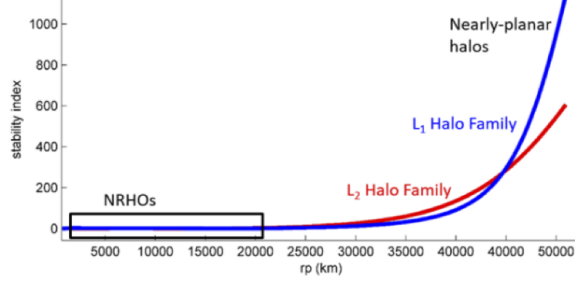


Figure 13: Earth-Moon L_1 and L_2 halo stability indices [3]

These orbits offer advantages such as relatively inexpensive transfer options from the Earth as well as feasible transfer options to the lunar surface and other orbits in cis-lunar space and beyond. The region of bounded stability index values defines the interval across the halo orbits that are debited as NRHOs, as shown in Figure 14. [1]

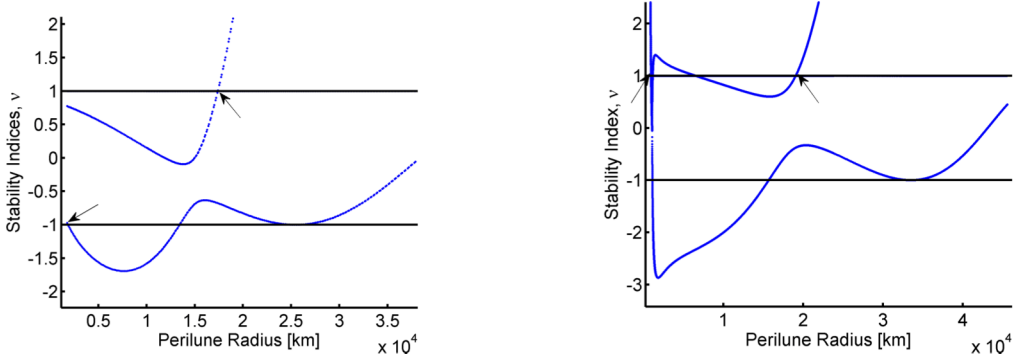


Figure 14: Earth-Moon L_1 (right) and L_2 (left) halo stability indices [1]

Some characteristics of the NRHOs concerning the perilune radii and the period are listed in Table 2.

	L1	L2
Perilune radius r_p	900 km - 19000 km	1850 km - 17350 km
Period T	8 - 10 days	6 - 10 days

Table 2: Orbital characteristics of NRHOs

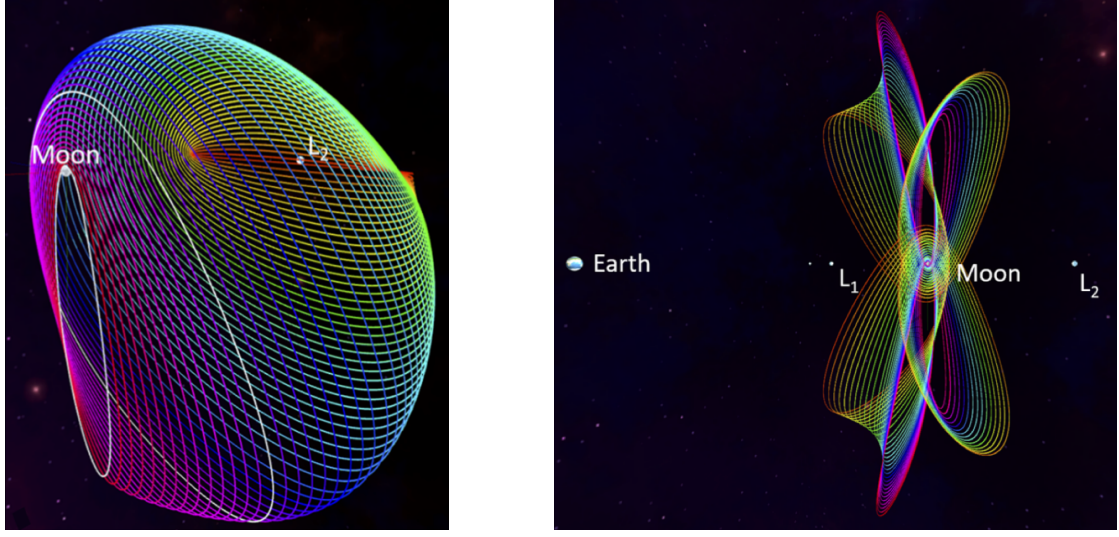


Figure 15: Bounds of NRHOs Figure 16: L_1 and L_2 northern and southern NRHOs [3]

3 Dynamical Models

3.1 n -Body Problem

The n -body problem of celestial mechanics deals with the prediction of the trajectories of n bodies under the influence of their mutual gravitation. The derivation of the equations of motion begins with n particles and the gravitational force due to a particle j

$$\bar{F}_i = -\frac{Gm_i m_j}{r_{ji}^2} \frac{\bar{r}_{ji}}{r_{ji}}, \quad (3)$$

where G is the universal gravitational constant and $i \neq j$.

With the law of motion $\bar{F}_i = m_i \ddot{r}_i$, assuming constant masses, the acceleration of the i^{th} particle, \ddot{r}_i , results from the sum of all n particles gravitational forces and becomes

$$\frac{d^2 \bar{r}}{dt^2} = \ddot{r}_i = -G \sum_{j=1, j \neq i}^n \frac{m_j \bar{r}_{ji}}{r_{ji}^2}. \quad (4)$$

3.2 Three Body Problem

The Three Body Problem (3BP) is a special case of the n -Body Problem with $n = 3$. The equations of motion thus result from (4) to

$$\ddot{r}_3 = -\frac{Gm_1}{r_{13}^2} \bar{r}_{13} - \frac{Gm_2}{r_{23}^2} \bar{r}_{23}. \quad (5)$$

Since there is no general closed-form solution for this problem, numerical methods or simplifications are needed to solve the equations. [4]

3.3 Circular Restricted Three Body Problem

3.3.1 Assumptions

The Circular Restricted Three Body Problem (CR3PB) is based on the Three Body Problem and can be solved exactly with the following assumptions [7]:

- One mass is much smaller than the other two, $m_3 \ll m_2, m_1$, so that the belonging motions of P_1 and P_2 are independent of P_3 .
- The primaries, P_1 and P_2 , move in circular, Keplerian orbits about their common barycenter.
- The bodies are only capable of translational motion and are assumed as point masses.

3.3.2 Coordinate Systems

The **Inertial Frame** I with the unit vectors \hat{X} , \hat{Y} and \hat{Z} is defined such that \hat{X} and \hat{Y} are in the plane of primary motion and $\hat{Z} = \hat{X} \times \hat{Y}$. A **Rotating Frame** R can be defined with the barycenter B of the primaries P_1 and P_2 as the origin, such that \hat{x} is always aligned with both primaries, \hat{y} is perpendicular to \hat{x} and in the plane of primary motion and $\hat{z} = \hat{Z}$. The frame R is rotating at a rate θ' relative to the inertial frame I . Due to the assumption of circular orbits of the primaries about the barycenter, θ' appears with a constant rate with $\theta = Nt$ and $\theta_0 = \theta(t_0) = 0$ at an initial time t_0 . The value N represents the mean motion.

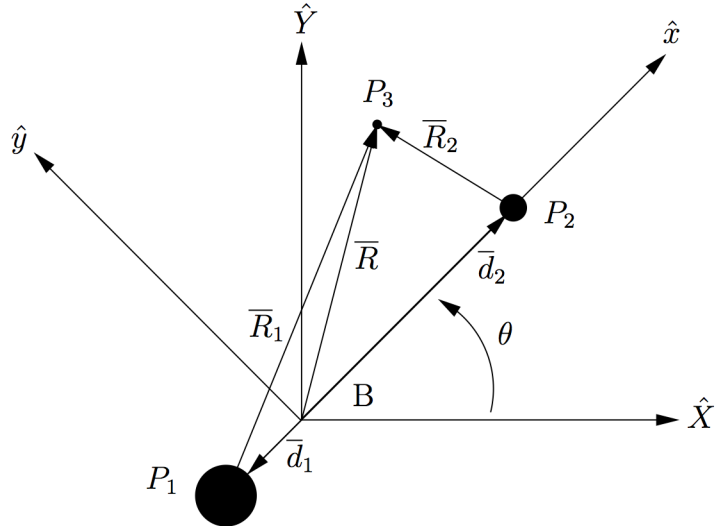


Figure 17: Reference frames and position vectors in the CR3BP [4]

With the position vectors defined in Figure 17, Equation 5 can be rewritten as

$$\frac{^I d^2 \bar{R}}{dt^2} = -\frac{GM_1}{R_1^3} \bar{R}_1 - \frac{GM_2}{R_2^3} \bar{R}_2. \quad (6)$$

Due to $\dot{\theta}$ having a constant value, vectors can be transformed between the frames using a simple direction cosine matrix:

$$\begin{pmatrix} X \\ Y \\ Z \end{pmatrix} = \begin{bmatrix} \cos \dot{\theta}t & -\sin \dot{\theta}t & 0 \\ \sin \dot{\theta}t & \cos \dot{\theta}t & 0 \\ 0 & 0 & 1 \end{bmatrix} \begin{pmatrix} x \\ y \\ z \end{pmatrix} \quad (7)$$

3.3.3 Non-dimensionalization

To generalize results and to improve numerical conditioning for integration, Equation 6 can be non-dimensionalized by introducing various characteristic quantities. These quantities include the characteristic length L^* , which is defined as the distance between the two primaries P_1 and P_2 , that is $L^* = |\bar{d}_1| + |\bar{d}_2|$. The characteristic mass M^* is defined as the sum of the masses of the primaries $M^* = m_1 + m_2$.

The characteristic time T^* is defined such that the nondimensional units of the gravitational constant G and the mean motion n equal to one:

$$T^* = \sqrt{\frac{l^{*3}}{Gm^*}} \quad (8)$$

3.3.4 Equations of Motion

Using these expressions from 3.3.3, the inertial acceleration vector for P_3 can be rewritten to

$$\frac{^I d^2 \bar{r}}{dt^2} = -\frac{(1-\mu)}{r_1^3} \bar{r}_1 - \frac{\mu}{r_2^3} \bar{r}_2, \quad (9)$$

where the position vectors are $\bar{r} = \frac{\bar{R}}{L^*}$, $\bar{r}_1 = \frac{\bar{R}_1}{L^*}$ and $\bar{r}_2 = \frac{\bar{R}_2}{L^*}$. The mass ratio μ is defined as $\mu = \frac{M_2}{M^*}$ and $(1-\mu) = \frac{M_1}{M^*}$. The position vector \bar{r} in the rotating frame R is defined as

$$\bar{r} = x\hat{x} + y\hat{y} + z\hat{z}. \quad (10)$$

The first and second derivative of this equation with respect to nondimesnional time and relative to an inertial observer become

$${}^I \dot{\bar{r}} = \frac{{}^I d \bar{r}}{dt} = \frac{{}^R d \bar{r}}{dt} + {}^I \bar{\omega}^R \times \bar{r}, \quad (11)$$

$${}^I \ddot{\bar{r}} = \frac{{}^I d {}^I \dot{\bar{r}}}{dt} = \frac{{}^R d {}^I \dot{\bar{r}}}{dt} + {}^I \bar{\omega}^R \times {}^I \dot{\bar{r}}, \quad (12)$$

where ${}^I\bar{\omega}^R = \dot{\theta}$ is the velocity of the rotating frame R with respect to the inertial frame I . Due to the assumption of circular orbits, this angular velocity is constant and equals

$${}^I\bar{\omega}^R = n\hat{z} = \begin{pmatrix} 0 \\ 0 \\ n \end{pmatrix}. \quad (13)$$

Since $\hat{z} = \hat{Z}$, (11) and (12) can then be evaluated and written as

$${}^I\dot{\vec{r}} = (\dot{x} - ny)\hat{x} + (\dot{y} + nx)\hat{y} + \dot{z}\hat{z}, \quad (14)$$

$${}^I\ddot{\vec{r}} = (\ddot{x} - 2n\dot{y} - n^2x)\hat{x} + (\ddot{y} + 2n\dot{x} - n^2y)\hat{y} + \ddot{z}\hat{z}. \quad (15)$$

Because of the definition of the mass ratio μ and the assumed circular motion of the primaries about their common barycenter, the nondimensional distances \bar{d}_1 and \bar{d}_2 can be written in the rotating frame R in the form

$$\bar{d}_1 = -\mu\hat{x}, \quad (16)$$

$$\bar{d}_2 = (1 - \mu)\hat{x}. \quad (17)$$

This leads to the components \bar{r}_1 and \bar{r}_2 :

$$\bar{r}_1 = \bar{r} - \bar{d}_1 = (x + \mu)\hat{x} + y\hat{y} + z\hat{z} \quad (18)$$

$$\bar{r}_2 = \bar{r} - \bar{d}_2 = (x - (1 - \mu))\hat{x} + y\hat{y} + z\hat{z} \quad (19)$$

The scalar equations, which comprise the dynamical model for the CR3BP, can then be written in the form

$$\begin{aligned} \ddot{x} - 2n\dot{y} - n^2x &= -\frac{(1 - \mu)(x + \mu)}{r_1^3} - \frac{\mu(x - (1 - \mu))}{r_2^3}, \\ \ddot{y} + 2n\dot{x} - n^2y &= -\frac{(1 - \mu)y}{r_1^3} - \frac{\mu y}{r_2^3}, \\ \ddot{z} &= -\frac{(1 - \mu)z}{r_1^3} - \frac{\mu z}{r_2^3}. \end{aligned} \quad (20)$$

Introducing the the pseudo-potential function U as

$$U = \frac{1 - \mu}{r_1} + \frac{\mu}{r_2} + \frac{1}{2}n^2(x^2 + y^2), \quad (21)$$

the scalar equations of motion can be rewritten in the form

$$\begin{aligned} \ddot{x} - 2n\dot{y} &= U_x, \\ \ddot{y} + 2n\dot{x} &= U_y, \\ \ddot{z} &= U_z, \end{aligned} \quad (22)$$

where U_j denotes $\frac{\partial U}{\partial j}$.

3.3.5 Jacobi Constant

In the rotating-frame formulation of the CR3BP exists one useful constant, which provides insight into the dynamical behavior in the CR3BP.

3.4 First Order Analytical Approximations for Motion in the Vicinity of Libration Points

There exist equilibrium solutions and solutions to the equations of motion for $\bar{\nabla}U = 0$, which determine the location of the libration points. To describe the motion in the vicinity of the libration point L_i , $i \in \{1, 2, 3, 4, 5\}$, with $(x_{L_i}, y_{L_i}, z_{L_i})$ as the position relative to the barycenter, a Taylor series expansion about L_i retaining only first-order terms is used to linearize the nonlinear system. The variational variables (ξ, η, ζ) are introduced such that $\xi = x - x_{L_i}$, $\eta = y - y_{L_i}$ and $\zeta = z - z_{L_i}$. This results in the linear variational equations for motion about L_i :

$$\ddot{\xi} - 2\dot{\eta} = U_{xx}^* \xi + U_{xy}^* \eta + U_{xz}^* \zeta, \quad (23)$$

$$\ddot{\eta} + 2\dot{\xi} = U_{yx}^* \xi + U_{yy}^* \eta + U_{yz}^* \zeta, \quad (24)$$

$$\ddot{\zeta} = U_{zx}^* \xi + U_{zy}^* \eta + U_{zz}^* \zeta, \quad (25)$$

where $U_{jk} = \frac{\partial U}{\partial j \partial k}$ and $U_{jk}^* = U_{jk}|_{L_i}$. With the state vector $\bar{\xi} \equiv [\xi \ \eta \ \zeta \ \dot{\xi} \ \dot{\eta} \ \dot{\zeta}]$, this system of three second-order differential equations can be written in state space form as

$$\dot{\bar{\xi}} = \mathbf{A}\bar{\xi}, \quad (26)$$

with

$$\mathbf{A} \equiv \begin{bmatrix} \mathbf{0} & \mathbf{I}_3 \\ \mathbf{B} & 2\mathbf{C} \end{bmatrix} = \begin{bmatrix} 0 & 0 & 0 & 1 & 0 & 0 \\ 0 & 0 & 0 & 0 & 1 & 0 \\ 0 & 0 & 0 & 0 & 0 & 1 \\ U_{xx}^* & U_{xy}^* & U_{xz}^* & 0 & 2 & 0 \\ U_{yx}^* & U_{yy}^* & U_{yz}^* & -2 & 0 & 0 \\ U_{zx}^* & U_{zy}^* & U_{zz}^* & 0 & 0 & 0 \end{bmatrix}. \quad (27)$$

and the submatrices

$$\mathbf{0} \equiv 3 \times 3 \quad \text{zero matrix}, \quad (28)$$

$$\mathbf{I}_3 \equiv 3 \times 3 \quad \text{identity matrix}, \quad (29)$$

$$\mathbf{B} \equiv \begin{bmatrix} U_{xx}^* & U_{xy}^* & U_{xz}^* \\ U_{yx}^* & U_{yy}^* & U_{yz}^* \\ U_{zx}^* & U_{zy}^* & U_{zz}^* \end{bmatrix}, \quad (30)$$

$$\mathbf{C} \equiv \begin{bmatrix} 0 & 1 & 0 \\ -1 & 0 & 0 \\ 0 & 0 & 0 \end{bmatrix}. \quad (31)$$

The solution to the system of linear differential equations is of the following form

$$\xi = \sum_{i=1}^6 A_i e^{s_i t}, \quad (32)$$

$$\eta = \sum_{i=1}^6 B_i e^{s_i t}, \quad (33)$$

$$\zeta = \sum_{i=1}^6 C_i e^{s_i t}, \quad (34)$$

where the six eigenvalues of the matrix \mathbf{A} appear as s_i and A_i , B_i and C_i represent coefficients. The eigenvalues determine the stability of the linear system for motion relative to the equilibrium points and therefore contain information about the stability of the nonlinear system.

Since two of the six eigenvalues are real, the motion surrounding the collinear libration points is generally unstable. However, the other four eigenvalues are purely imaginary, indicating the potential for strictly oscillatory motion. It is therefore possible to select initial conditions that excite only the oscillatory modes and generate stable periodic orbits.

3.5 Approximate Periodic Solutions

For these initial conditions mentioned above, the general form of the solution for motion near the collinear libration points can be expressed in the form

$$\xi = A_1 \cos \lambda t + A_2 \sin \lambda t, \quad (35)$$

$$\eta = -kA_1 \sin \lambda t + kA_2 \cos \lambda t. \quad (36)$$

λ represents the in-plane frequency, ν is the out-of-plane frequency and k is a constant denoting a relationship between the coefficients corresponding to the ξ and η components. The out-of-plane linearized motion is simple harmonic and can be described as

$$\zeta = C_1 \sin \nu t + C_2 \cos \nu t. \quad (37)$$

This leads to a quasi-periodic motion, because the ratio of the in-plane frequency and the out-of-plane frequency $\frac{\lambda}{\nu}$ is generally irrational. The equations therefore describe Lissajous type trajectories.

Halo-type periodic motion can be obtained for amplitudes of the in-plane and out-of-plane motions being of sufficient magnitude so that the non-linear contributions to the system produce eigenfrequencies that are equal. This solution can then be expressed in the form

$$\xi = -A_x \cos \lambda t + \phi, \quad (38)$$

$$\eta = kA_x \sin \lambda t + \phi, \quad (39)$$

$$\zeta = A_z \sin \nu t + \psi, \quad (40)$$

where Ax and Az are the in-plane and out-of-plane amplitudes, while ψ and ϕ are the phase angles. An initial guess that is near a periodic orbit for generating an exact numerically integrated solution to the nonlinear equations can sometimes be provided by an approximate analytical solution.

4 Dynamical Systems Theory

4.1 State Transition Matrix

In 4.2 a numerical technique to determine periodic orbits in the nonlinear system will be described. This method of differential corrections requires information concerning the sensitivity of a state along the path to changes in the initial conditions. This information can be found by linearizing the equations of motion relative to a reference trajectory, i.e, one that is a solution to the nonlinear differential equations. By introducing perturbation variables, the six-dimensional state vector is then defined as

$$\delta\bar{x} \equiv [\delta x \quad \delta y \quad \delta z \quad \delta\dot{x} \quad \delta\dot{y} \quad \delta\dot{z}]^T. \quad (41)$$

The resulting state space form can be written as

$$\delta\dot{\bar{x}} = \mathbf{A}(t)\delta\bar{x}(t), \quad (42)$$

with the time-dependent matrix

$$\mathbf{A}(t) \equiv \begin{bmatrix} \mathbf{0} & \mathbf{I}_3 \\ \mathbf{B}(t) & \mathbf{C} \end{bmatrix}. \quad (43)$$

This matrix is similar in form to the \mathbf{A} matrix of 3.4, with the difference of the submatrix $\mathbf{B}(t)$ being time-varying and not a constant. The general form solution to Equation 42 is

$$\delta\bar{x}(t) = \Phi(t, t_0)\delta\bar{x}(t_0) \quad (44)$$

where $\Phi(t, t_0)$ is the state transition matrix (STM). The STM is a linear map from the initial state at the initial time t_0 to a state at some later time t and therefore offers a tool to approximate the impact of variations in the initial state on the evolution of the trajectory. The STM must satisfy the matrix differential equation

$$\dot{\Phi}(t, t_0) = \mathbf{A}(t)\Phi(t, t_0), \quad (45)$$

given the initial condition,

$$\Phi(t_0, t_0) = I_6. \quad (46)$$

The STM can be determined as a function of time by integrating Equation 45 from the initial value in Equation 46 simultaneously with the system equations of motion

in Equation 22. For numerical simulation, the scalar equations of motion in must be rewritten as the following set of six first-order differential equations: [4]

$$\begin{aligned}\dot{r}_x &= v_x \\ \dot{r}_y &= v_y \\ \dot{r}_z &= v_z \\ \dot{v}_x &= 2\dot{r}_y + \frac{\partial U}{\partial x} \\ \dot{v}_y &= -2\dot{r}_x + \frac{\partial U}{\partial y} \\ \dot{v}_z &= \frac{\partial U}{\partial z}\end{aligned}\tag{47}$$

Each element of the STM predicts how the elements of the final state change based on changes in the initial state. The STM is defined as

$$\Phi(t, t_0) = \frac{\partial \bar{x}(t)}{\partial \bar{x}_0} = \begin{bmatrix} \frac{\partial x}{\partial x_0} & \frac{\partial x}{\partial y_0} & \frac{\partial x}{\partial z_0} & \frac{\partial x}{\partial \dot{x}_0} & \frac{\partial x}{\partial \dot{y}_0} & \frac{\partial x}{\partial \dot{z}_0} \\ \frac{\partial y}{\partial x_0} & \frac{\partial y}{\partial y_0} & \frac{\partial y}{\partial z_0} & \frac{\partial y}{\partial \dot{x}_0} & \frac{\partial y}{\partial \dot{y}_0} & \frac{\partial y}{\partial \dot{z}_0} \\ \frac{\partial z}{\partial x_0} & \frac{\partial z}{\partial y_0} & \frac{\partial z}{\partial z_0} & \frac{\partial z}{\partial \dot{x}_0} & \frac{\partial z}{\partial \dot{y}_0} & \frac{\partial z}{\partial \dot{z}_0} \\ \frac{\partial \dot{x}}{\partial x_0} & \frac{\partial \dot{x}}{\partial y_0} & \frac{\partial \dot{x}}{\partial z_0} & \frac{\partial \dot{x}}{\partial \dot{x}_0} & \frac{\partial \dot{x}}{\partial \dot{y}_0} & \frac{\partial \dot{x}}{\partial \dot{z}_0} \\ \frac{\partial \dot{y}}{\partial x_0} & \frac{\partial \dot{y}}{\partial y_0} & \frac{\partial \dot{y}}{\partial z_0} & \frac{\partial \dot{y}}{\partial \dot{x}_0} & \frac{\partial \dot{y}}{\partial \dot{y}_0} & \frac{\partial \dot{y}}{\partial \dot{z}_0} \\ \frac{\partial \dot{z}}{\partial x_0} & \frac{\partial \dot{z}}{\partial y_0} & \frac{\partial \dot{z}}{\partial z_0} & \frac{\partial \dot{z}}{\partial \dot{x}_0} & \frac{\partial \dot{z}}{\partial \dot{y}_0} & \frac{\partial \dot{z}}{\partial \dot{z}_0} \end{bmatrix}.\tag{48}$$

The State Transition Matrix evaluated over precisely one orbital period, $\Phi(t_0 + P, t_0)$ is called **Monodromy Matrix**. The eigenvalues of the Monodromy Matrix are used to assess the stability characteristics of a periodic orbit in a linear sense.

4.2 Differential Corrections

The Differential Corrections method is a numerical, iterative technique which uses the information from the STM and a reference trajectory in order to achieve a desired result. In this context its objective is the generation of a trajectory that terminates at a desired state $\bar{x}(t_f)_{des}$. Integrating $\bar{x}(t_0)$ will terminate at some state $\bar{x}(t_f)$ which differs from the desired state. The initial guess is then updated until certain convergence criteria are met by minimizing the error between the desired and actual final state, $\delta x(t_i)$. [8]

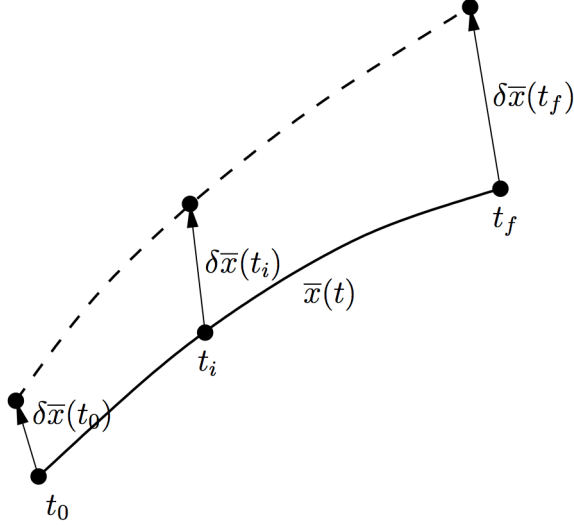


Figure 18: Linear variations relative to a reference trajectory $\bar{x}(t)$

The algorithm for the implementation of a shooting method allows for the manipulation of design variables to satisfy a set of given constraints. The free variable vector is defined as

$$\bar{X} = \begin{pmatrix} X_1 \\ X_2 \\ \vdots \\ X_n \end{pmatrix} \quad (49)$$

with the elements of X being the n design variables that are allowed to be modified. They usually include state elements, integration times, epochs, and other quantities. This vector is subject to m constraint equations of the form

$$\bar{F}(\bar{X}) = \begin{pmatrix} F_1(\bar{X}) \\ F_2(\bar{X}) \\ \vdots \\ F_m(\bar{X}) \end{pmatrix} = 0 \quad (50)$$

The constraints are typically position, time of flight, or velocity constraints, although many other types of constraints are possible. The objective of this Free-Variable Formulation of the Differential Corrections Method is the determination of a design vector \bar{X} , that satisfies $\bar{F}(\bar{X}) = 0$. An iterative process to solve for \bar{X} , given an initial guess for the free variable vector \bar{X}_0 , is derived by expanding the constraint vector in a Taylor series about

the initial guess:

$$\bar{F}(\bar{X}) = \bar{F}(\bar{X}_0) + \frac{\partial \bar{F}(\bar{X}_0)}{\partial \bar{X}_0} (\bar{X} - \bar{X}_0) + H.O.T.s \quad (51)$$

$$0 \approx \bar{F}(\bar{X}_0) + \frac{\partial \bar{F}(\bar{X}_0)}{\partial \bar{X}_0} (\bar{X} - \bar{X}_0) \quad (52)$$

$\frac{\partial \bar{F}(\bar{X}_0)}{\partial \bar{X}_0}$ is an $m \times n$ matrix typically denoted as the Jacobian Matrix

$$D\bar{F}(\bar{X}_0) = \frac{\partial \bar{F}(\bar{X}_0)}{\partial \bar{X}_0} = \begin{bmatrix} \frac{\partial F_1}{\partial X_1} & \frac{\partial F_1}{\partial X_2} & \cdots & \frac{\partial F_1}{\partial X_n} \\ \frac{\partial F_2}{\partial X_1} & \frac{\partial F_2}{\partial X_2} & \cdots & \frac{\partial F_2}{\partial X_n} \\ \vdots & \vdots & \ddots & \\ \frac{\partial F_m}{\partial X_1} & \frac{\partial F_m}{\partial X_2} & \cdots & \frac{\partial F_m}{\partial X_n} \end{bmatrix}. \quad (53)$$

Equation 52 can be written in an iterative update form:

$$n = m : \quad \bar{X}_{j+1} = \bar{X}_j - D\bar{F}(\bar{X}_j)^{-1} \bar{F}(\bar{X}_j) \quad (54)$$

$$n > m : \quad \bar{X}_{j+1} = \bar{X}_j - D\bar{F}(\bar{X}_j)^T [D\bar{F}(\bar{X}_j) \cdot D\bar{F}(\bar{X}_j)^T]^{-1} \bar{F}(\bar{X}_j) \quad (55)$$

Equation 54 is a multi-dimensional form of the well-known Newton's method. In summary, the general structure of the constraint and free variable formulation allows four basic steps:

1. Select the free-variables and construct the $n \times 1$ design variable vector \bar{X} with an initial value \bar{X}_0 .
2. Define constraints as equality constraints and formulate the $m \times 1$ constraint vector $\bar{F}(\bar{X}) = 0$.
3. Compute the partial derivatives of the constraint vector with respect to each of the design variables and assemble the results into the $m \times n$ Jacobian matrix $D\bar{F}(\bar{X})$.
4. Depending upon the relationship between m and n , use either equation Equation 54 or Equation 55 to compute \bar{X}_{j+1} . The new \bar{X}_{j+1} vector then is defined as the reference \bar{X}_j and the process repeats until $\bar{F}(\bar{X}_{j+1}) < \epsilon$. [9]

4.3 Periodic Halo Orbit Computation

Halo orbits are three-dimensional orbits and periodic in the CR3BP. They can be computed using either a single oder multiple shooting scheme as described in 4.2. Due to the symmetry of halo orbits across the xz-plane, a single shooting algorithm serves as the basis for a simple and efficient corrections process to compute the trajectory.

Since every correction method requires an initial guess, the intersection point of the

xz -plane serves as a good starting point due the orbits symmetry. As a result, $y_0 = \dot{x}_0 = \dot{z}_0 = 0$ and the state vector of the initial state x_0 becomes

$$x_0 = [x_0 \ 0 \ z_0 \ 0 \ \dot{y}_0 \ 0]^T. \quad (56)$$

The free variable vector \bar{X} for the differential corrections method can then be written as

$$\bar{X} = \begin{pmatrix} x_0 \\ z_0 \\ \dot{y}_0 \\ T \end{pmatrix} \quad (57)$$

The time T is included to implement a variable-time shooting algorithm. The constraints on the state variables used to enforce a perpendicular xz -plane crossing are then defined as

$$\bar{F}(\bar{X}) = \begin{pmatrix} y(T) \\ \dot{x}(T) \\ \dot{z}(T) \end{pmatrix} = 0 \quad (58)$$

The Jacobian matrix $D\bar{F}(\bar{X})$ can be expressed by

$$D\bar{F}(\bar{X}) = \begin{bmatrix} \frac{\partial y}{\partial x_0} & \frac{\partial y}{\partial z_0} & \frac{\partial y}{\partial \dot{y}_0} & \dot{y}(T) \\ \frac{\partial \dot{x}}{\partial x_0} & \frac{\partial \dot{x}}{\partial z_0} & \frac{\partial \dot{x}}{\partial \dot{y}_0} & \ddot{x}(T) \\ \frac{\partial \dot{z}}{\partial x_0} & \frac{\partial \dot{z}}{\partial z_0} & \frac{\partial \dot{z}}{\partial \dot{y}_0} & \ddot{z}(T) \end{bmatrix}. \quad (59)$$

The first three columns are elements of the STM $\phi(T, 0)$ and the elements of the last column are evaluated at the final time. These equations can now be used within the differential corrections method to compute halo orbits. [7]

4.4 Continuation of an Halo Orbit Family

Single and multiple shooting schemes offer one single point solutions for a trajectory based on the initial state. The following strategies are possibilities to compute families of orbits.

4.4.1 Natural Parameter Continuation

The natural parameter continuation is a simple strategy based on a single converged solution to find and construct a family of orbits, i.e. a family of related solutions. As described in 4.2, the single converged solution can be found by single shooting. One parameter associated with this solution (e.g. x_0, y_0, z_0, T or Jacobi constant, among many other possibilities) is incremented by a small, specific amount. The modified solution is then employed as an initial guess for a new trajectory in a differential corrections scheme. This process is repeated to construct the family of related solutions. As an example, a continuation scheme with increments in x_0 is shown for a halo orbit:

1. A converged solution was found with the initial state $\bar{x}_{0,j}^* = [x_{0,j} \ 0 \ z_{0,j} \ 0 \ \dot{y}_{0,j} \ 0]^T$ and the period P_j . The superscript * refers to a converged solution while no superscript implies an initial guess.
2. By incrementing x_0 by a small step β , the initial guess for a nearby solution results in $\bar{x}_{0,j+1} = [(x_{0,j} + \beta) \ 0 \ z_{0,j} \ 0 \ \dot{y}_{0,j} \ 0]^T$.
3. The initial guess $\bar{x}_{0,j+1}$ is now used in a differential corrections scheme. The x -coordinate is not allowed to be included in the free variable vector \bar{X} , as the solution could re-converge onto $\bar{x}_{0,j}^*$.
4. The correction process converges on a nearby solution with the initial state $\bar{x}_{0,j+1}^* = [(x_{0,j} + \beta) \ 0 \ z_{0,j+1} \ 0 \ \dot{y}_{0,j+1} \ 0]^T$ with the period P_{j+1} .
5. The process is repeated to continue the family.

Due to the many modifiable parameters and the different selectable step size β , the continuation requires some intuition concerning the evolution of the family. [7]

4.4.2 Pseudo-Arclength Continuation

The Pseudo-Arclength Continuation method is an alternative continuation scheme, which avoids the required intuition concerning the evolution of the family necessary for the Natural Parameter Continuation. The increment Δs is defined in a direction tangent to the family. Therefore all free variables are updated simultaneously by stepping in a tangent direction of the free variable vector of a converged solution.

Given a free variable vector of a previously converged solution \bar{X}_j^* , a unit vector tangent to the family at \bar{X}_j^* is constructed from the null vector of the Jacobian matrix $D\bar{F}(\bar{X}_j^*)$, denoted $\Delta\bar{X}_j^*$. As an additional constraint to the original constraint vector $\bar{F}(\bar{X}_{j+1})$, the scalar pseudo-arclength constraint, is defined as

$$(\bar{X}_{j+1} - \bar{X}_j^*)^T \Delta\bar{X}_j^* - \Delta s = 0. \quad (60)$$

The augmented constraint vector is then

$$\bar{G}(\bar{X}_{j+1}) = \begin{bmatrix} \bar{F}(\bar{X}_{j+1}) \\ (\bar{X}_{j+1} - \bar{X}_j^*)^T \Delta\bar{X}_j^* - \Delta s \end{bmatrix} = 0 \quad (61)$$

The derivative of the augmented constraint vector $\bar{G}(\bar{X}_{j+1})$ yields an augmented Jacobian matrix, given by

$$D\bar{G}(\bar{X}_{j+1}) = \frac{\partial \bar{G}(\bar{X}_{j+1})}{\partial \bar{X}_{j+1}} = \begin{bmatrix} D\bar{F}(\bar{X}_{j+1}) \\ \Delta\bar{X}_j^{*T} \end{bmatrix} \quad (62)$$

Using the constructed augmented constraint vector and Jacobian matrix, an iterative Newton's method is used to converge on the next family member \bar{X}_{j+1}^* . [7]

References

- [1] E. M. Zimovan, “Near rectilinear halo orbits and their application in cis-lunar space,”
- [2] K. C. Howell, “Three-dimensional, periodic, ’halo’ orbits,” 1983.
- [3] D. Davis, “Orbit maintenance and navigation of human spacecraft at cislunar near rectilinear halo orbits,”
- [4] D. P. Gordon, “Transfers to earth-moon l2 halo orbits using lunar proximity and invariant manifolds,” 2008.
- [5] E. Kolemen, “Quasi-periodic orbits of the restricted three-body problem made easy,”
- [6] “Distant Retrograde Orbits.” http://ccar.colorado.edu/asen5050/projects/projects_2013/Johnson_Kirstyn/finalorbit.html. Accessed: 2017-12-05.
- [7] E. M. Zimovan, “Characteristics and design strategies for near rectilinear halo orbits within the earth-moon system,” 2017.
- [8] A. MacInnes, “An introduction to libration point orbits,” 2009.
- [9] R. E. Pritchett, “Numerical methods for low-thrust trajectory optimization,” 2016.